80 Journal of Air-Conditioning and Refrigeration Volume 6 August(1998)/pp. 80~92

A Third-order Simulation Model of a Vuilleumier Cycle Heat Pump

Young-Goo Kang* and Eun-Soo Jeong**

Key Words : Vuilleumier or VM, Heat pump, Major losses, Performance analysis, Third-order analysis, Heating capacity, Cooling capacity, COP

Abstract

A third-order simulation model of a Vuilleumier(VM) heat pump has been developed. This model takes into account the major losses such as the heat conduction losses through regenerators and displacers, the pumping losses and the wall-to-gas heat transfer losses in active volumes, in addition to the heat exchanger and regenerator losses. The working volume was divided into 12 control volumes and the conservation equations of mass and energy were applied to each control volume. Pressure drops were considered in regenerators only. Thermodynamic behavior of the working gas in a VM heat pump was investigated and effects of the major losses and operating conditions on the performance of a VM heat pump were shown.

Nomenclature

A	: Cross sectional area
A_{wg}	: Heat transfer area
C_p	: Specific heat for constant pressure
C_v	: Specific heat for constant volume
COP_c	: Coefficient of performance for cooling
COP_h	: Coefficient of performance for heating
d_h	: Hydraulic diameter
f_r	: Reynolds friction factor
h	: Heat transfer coefficient
$\dot{H}_{pump,i}$	: Enthalpy flow into control volume (i) from appendix gap
k	: Thermal conductivity
L	: Length
M	: Mass
$\dot{m}_{ij}$	: Mass flow rate from control volume (i) to control volume (j)
P	: Pressure
Pr	: Prandtl number
$\dot{Q}$	: Heat transfer rate
$\overline{\dot{Q}}$	: Net heat transfer rate
R	: Gas constant

* Sindo Ricoh, 277-22 Sungsudong, Sungdongku, Seoul 133-705, Korea
** Department of Mechanical Engineering, Hongik University, 72-1 Sangsudong, Mapoku, Seoul 121-791, Korea

Re_h : Reynolds number
T : Temperature
$\overline{T}$: Time-averaged temperature
t : Time
V : Volume
$\dot{W}_{shaft}$: Net shaft work rate

Greek letters

γ : Specific heat ratio
φ : Porosity of a regenerator
ω : Angular velocity
μ : Viscosity

Subscripts

AH : Hot-side warm heat exchanger
ah : Hot-side warm active volume
AHRH : From hot-side warm heat exchanger to hot regenerator
AK : Cold-side warm heat exchanger
ak : Cold-side warm active volume
app : Appendix gap
cond : Heat conduction
disp : Displacer
f : Interface between control volumes
H : Hot heat exchanger
h : Hot active volume
i : Number of a control volume
K : Cold heat exchanger
k : Cold active volume
KRK : From cold heat exchanger to cold regenerator
pump : Pumping loss
RHH : From hot regenerator to hot heat exchanger
*RH*1 : Hot regenerator 1
*RH*12 : Hot regenerator 1 and 2
*RH*2 : Hot regenerator 2
RKAK : From cold regenerator to cold-side warm heat exchanger
*RK*1 : Cold regenerator 1
*RK*12 : Cold regenerator 1 and 2
*RK*2 : Cold regenerator 2
w : Wall

1. Introduction

Vuilleumier (VM) heat pumps are heat-driven devices which can be used for both cooling and heating. VM heat pumps are driven by natural gas or waste heat instead of electricity so that they can reduce the electric peak load during the summer. Also, VM heat pumps can avoid the CFC regulations since they use helium gas as a working fluid. Other attractive features of VM heat pumps are high theoretical COP's, low noise, long life and less dependence of heating capacity on outdoor temperature than vapor compression heat pumps. The VM cycle has been used for small cryocoolers in the past due to its high reliability. Recently, efforts to develop VM heat pumps for residential use are being done. (Kang, 1992; Yoo and Kang, 1992; Kuehl et al., 1986; Carlsen, 1989)

Performance analysis models of VM heat pumps can be categorized into three types; first-order models such as the isothermal analysis and the adiabatic analysis, second-order models which correct the results of first-order models by considering the effects of various heat losses and pressure drops, and third-order models which directly calculate the effects of the limited heat transfer rates and the flow friction in heat exchangers and regenerators on the performance of VM heat pumps (Sekiya and Terada, 1991). The isothermal analysis, in which the temperature of each active volume is assumed to be equal to that of an adjacent heat exchanger, gives the highest COP's of VM heat pumps, but its results show large difference from those of actual VM heat pumps. Yoo(1989) proposed

an approximate solution for the adiabatic model of VM heat pumps assuming that the volume of each active volume varies linearly during arbitrary thermodynamic processes. Using this approximate solution Yoo and Kang (1992) proposed the preliminary design conditions of a VM refrigerator. Choi and Jeong (1996) proposed a second-order simulation model of VM heat pumps, in which the results of the adiabatic analysis were corrected by considering the various losses such as the enthalpy dump, the reheat loss, the pumping loss, the conduction loss and the shuttle heat transfer loss. Sherman(1971) and Kuehl et al. (1990) proposed simplified third-order analysis models of VM refrigerators and heat pumps, respectively, in which heat exchangers were included into adjacent active volumes. Sekiya and Terada(1991) applied a third-order analysis model of Stirling engines/refrigerators to VM heat pumps and compared the predictions with experimental results.

Since heating capacity, cooling capacity and COP's are considerably affected by various losses, first-order analysis models cannot predict the performance of a VM heat pump precisely (Kuehl et al., 1986). Second-order analysis models are suitable for use in parametric sensitivity analysis as required for design optimization due to their short simulation time. But, a third-order analysis model should be used to predict the performance of a VM heat pump accurately, although they require considerable computer time.

Existing third-order models considered only the losses due to the limited heat transfer rates and the pressure drops within heat exchangers and regenerators. In this study a third-order simulation model of a VM heat pump was proposed which takes the major losses into account. The losses due to the heat transfer between the working fluid and the wall of active volumes, the heat conductions through regenerators and displacers and the pumping losses are included in this model. Using this model, the effects of various losses and the operating conditions on the performance of a VM heat pump were investigated.

2. Mathematical Model

Figure 1 shows the schematic diagram of a VM heat pump. The working volume occupied by the working gas was divided into 12 control volumes as shown in Fig.1. A control volume was alloted to each active volume and heat exchanger, but each regenerator was divided into two control volumes because the axial temperature gradient was large within a regenerator. The appendix gap volumes in the hot and cold active volumes were considered to calculate the pumping losses.

Major assumptions used in the model are as follows:

1) The working gas is an ideal gas and

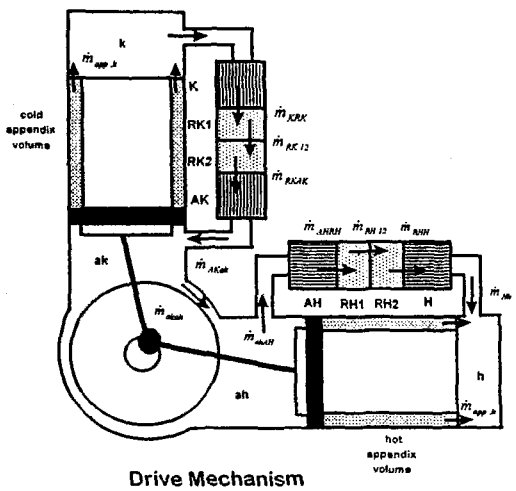

Fig.1 Schematic of a VM heat pump

the total mass of the working gas in a VM heat pump is constant.

2) Kinetic energy of the working gas is negligible.

3) The working gases within heat exchangers and active volumes can exchange heat externally, but the working gases within regenerators exchange heat with regenerator matrices only.

4) Cyclic steady state is established.

5) The temperature and pressure distributions within regenerators are linear.

6) Pressure drop occurs only in regenerators, and the pressure drops in heat exchangers and active volumes are negligible.

Control volume (i) in Fig.2 stands for any control volume in Fig.1. The energy conservation equation for the control volume (i) can be written as follows.

$$\frac{d(M_i C_v T_i)}{dt} = \dot{Q}_{w,i} + \dot{H}_{pump,i} + \dot{Q}_{cond,i} + \dot{m}_i C_p T_{f,i} - \dot{m}_{i+1} C_p T_{f,i+1} - P_i \frac{dV_i}{dt} \quad (1)$$

$T_{f,i}$ denotes the working gas temperature at the interface between the control volumes and takes the temperature of the upstream control volume. But, the working gas temperature at the interface between the regenerator control volumes is obtained by linear interpolation of the working gas temperature of adjacent control volumes since the axial temperature gradient is assumed to be linear within the regenerators. Substituting ideal gas equation into Eq. (1) gives the following equation.

$$\frac{C_v}{R} V_i \frac{dP_i}{dt} = \dot{Q}_{w,i} + \dot{H}_{pump,i} + \dot{Q}_{cond,i} + \dot{m}_i C_p T_{f,i} - \dot{m}_{i+1} C_p T_{f,i+1} - \frac{C_p}{R} P_i \frac{dV_i}{dt} \quad (2)$$

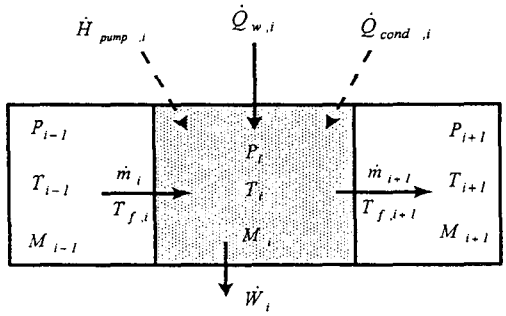

Fig.2 Control Volume (i)

$\dot{H}_{pump,i}$ denotes the enthalpy flow from an appendix gap into an adjacent active volume and considered only in the hot and cold active volumes. It can be expressed as:

$$\dot{H}_{pump,i} = \dot{m}_{app,i} C_p T_{app,i} \quad (3)$$

The mass flow rate and temperature of the working gas flowing into the hot active volume from the appendix gap can be ob-tained from the following equations (Choi et al., 1994).

$$\dot{m}_{app,h} = -\frac{V_{app} \ln(\overline{T}_h / \overline{T}_{ah})}{R(\overline{T}_h - \overline{T}_{ah})} \frac{dP_{app}}{dt} \quad (4.a)$$

$$T_{app,h} = \overline{T}_h - \frac{\overline{T}_h - \overline{T}_{ah}}{2L} X_d (1 - \sin \omega t) \quad (4.b)$$

Here, X_d denotes a half of the piston stroke.

$\dot{Q}_{w,i}$ is the heat transfer rate from the wall of an active volume or heat exchanger to the working gas, but it is the heat transfer rate from a regenerator matrix to the working gas in a regenerator. The heat transfer rate from the wall of an active volume to the working gas is obtained from the heat transfer relation proposed by Jeong and Smith.(1992)

$$\dot{Q}_{w,i} = A_{wg,i}(t) \frac{k}{H} \left[K_S (T_{w,i} - T_i(t)) + K_T \frac{H^2}{k} \frac{dP_i}{dt} \right] \quad (5)$$

Here, H denotes the radius of a cylinder. The heat transfer rates within heat exchangers and regenerators can be expressed as follows.

$$\dot{Q}_{w,i} = h_i A_{wg} (T_{w,i} - T_i) \tag{6}$$

Heat transfer coefficients for heat exchangers are calculated from the heat transfer relation by Urieli and Berchowitz (1984), and heat transfer coefficients for regenerators are calculated from the heat transfer relation by Tanaka et al. (1989)

$\dot{Q}_{cond,i}$ is the heat transfer rate flowing into control volume (i) by heat conduction. It is considered in heat exchangers and active volumes since the axial temperature gradient in regenerators and displacers are large. The heat conduction loss through the hot regenerator can be expressed as follows.

$$\dot{Q}_{cond,H} = -\left(\frac{kA}{L}\right)_{RH} (T_H - T_{AH}) \tag{7}$$

The heat conduction loss through the hot displacer can be given as:

$$\dot{Q}_{cond,h} = -\left(\frac{kA}{L}\right)_{disp.H} (T_h - T_{ah}) \tag{8}$$

According to assumption (6), pressure drop occurs in regenerators only. Hence, the cold active volume and the cold heat exchanger have the same pressure, P_k. From the energy conservation equations for cold active volume and cold heat exchanger we can get the time rate of the pressure variation within the cold active volume as follows.

$$\frac{dP_k}{dt} = \frac{\gamma-1}{A(t)} \left[\dot{Q}_{w,k} + \dot{Q}_{w,K} + \dot{Q}_{cond,k} + \dot{Q}_{cond,K} - \dot{m}_{KRK} C_p T_{KRK} - \frac{\gamma}{\gamma-1} P_k \frac{dV_k}{dt} \right] \tag{9.a}$$

$$A(t) = V_k + V_K + \frac{V_{app.k} \ln(\overline{T}_k / \overline{T}_{ak})}{\gamma(\overline{T}_k - \overline{T}_{ak})} T_{app.k} \tag{9.b}$$

The warm active volumes and the warm heat exchangers have the same pressure, P_a. The time rate of the pressure variation within the warm active volumes and the warm heat exchangers can be obtained from the energy conservation equations for the warm active volumes and the warm heat exchangers.

$$\frac{dP_a}{dt} = \frac{\gamma-1}{B(t)} \left[\dot{Q}_{w,AK} + \dot{Q}_{w,ak} + \dot{Q}_{w,ah} + \dot{Q}_{w,AH} + \dot{Q}_{cond,ak} + \dot{Q}_{cond,AK} + \dot{Q}_{cond,ah} + \dot{Q}_{cond,AH} + \dot{m}_{RKAK} C_p T_{RKAK} - \dot{m}_{AHRH} C_p T_{AHRH} - \frac{\gamma}{\gamma-1} \left\{ P_a \frac{dV_{ak}}{dt} + P_a \frac{dV_{ah}}{dt} \right\} \right] \tag{10.a}$$

$$B(t) = V_{AK} + V_{ak} + V_{ah} + V_{AH} \tag{10.b}$$

Time rate of the pressure variation within the hot active volume and the hot heat exchanger can be obtained similarly.

$$\frac{dP_h}{dt} = \frac{\gamma-1}{C(t)} \left[\dot{Q}_{w,H} + \dot{Q}_{w,h} + \dot{Q}_{cond,h} + \dot{Q}_{cond,H} + \dot{m}_{RHH} C_p T_{RHH} - \frac{\gamma}{\gamma-1} P_h \frac{dV_h}{dt} \right] \tag{11.a}$$

$$C(t) = V_H + V_h + \frac{V_{app.h} \ln(\overline{T}_h / \overline{T}_{ah})}{\gamma(\overline{T}_h - \overline{T}_{ah})} T_{app.h} \tag{11.b}$$

Out of twelve energy conservation equations for twelve control volumes shown in Fig.1, three equations are used to obtain P_h, P_a and P_k. Remaining nine energy conservation equations and two pressure drop equations through regenerators are used to ob-

tain eleven mass flow rates through the interfaces between control volumes

Pressure drops through regenerators are calculated by the relation proposed by Tanaka et al.(1989) According to Tanaka et al.(1989), the pressure drop through a regenerator can be expressed as follows.

$$\triangle P = 2f_r \frac{\mu L_i^2}{d_h^2 M_i} \dot{m}_i \tag{12.a}$$

$$f_r = \frac{f_h}{4} \mathrm{Re_h} = \frac{1}{4}\left(\frac{175}{\mathrm{Re_h}} + 1.6\right)\mathrm{Re_h} \tag{12.b}$$

$$\mathrm{Re_h} = \left|\frac{\dot{m} d_h}{\mu A \varphi}\right| \tag{12.c}$$

Here, φ is the porosity of a regenerator. The mass flow rates flowing through the middle sections of hot regenerator and cold regenerator are obtained from the following relations, respectively.

$$\dot{m}_{RK12} = \frac{\triangle P_{RK12}\, d_h^2\, M_{RK12}}{2\mu f_r\, L_{RK12}^2} \tag{13}$$

$$\dot{m}_{RH12} = \frac{\triangle P_{RH12}\, d_h^2\, M_{RH12}}{2\mu f_r\, L_{RH12}^2} \tag{14}$$

Time rate of the mass variation within each control volume can be obtained from the mass conservation equation for each control volume.

$$\frac{dM_i}{dt} = \dot{m}_i - \dot{m}_{i+1} \tag{15}$$

Equation (15) is applied to the control volumes other than the hot active volume to calculate the masses of control volumes. The mass of the hot active volume is calculated from the following relation, which ensures that the total mass of the working gas within a VM heat pump is constant.

$$M_h = M_{total} - (M_k + M_K + \ldots + M_{RH2} + M_H) \tag{16}$$

Since the pressure and the mass of each control volume can be determined from Eq. (9), (10), (11), (15) and (16), the working gas temperature within each control volume is obtained from the ideal gas relation.

$$T_i = \frac{P_i V_i}{M_i R} \tag{17}$$

The temperature of a matrix within a regenerator can be obtained from the energy conservation equation for each matrix.

$$\frac{dT_{w,i}}{dt} = -\frac{\dot{Q}_{w,i}}{(M_w)_i C_w} \tag{18}$$

Heating and cooling coefficients of performance which take the shaft work into account are expressed as:

$$COP_h = \frac{-\overline{\dot{Q}}_{w,AK} - \overline{\dot{Q}}_{w,AH}}{\overline{\dot{Q}}_{w,H} + \overline{\dot{Q}}_{w,h} + \overline{\dot{W}}_{shaft}} \tag{19}$$

$$COP_c = \frac{\overline{\dot{Q}}_{w,K}}{\overline{\dot{Q}}_{w,H} + \overline{\dot{Q}}_{w,h} + \overline{\dot{W}}_{shaft}} \tag{20}$$

$$\overline{\dot{W}}_{shaft} = -\left[\overline{\dot{Q}}_{w,AK} + \overline{\dot{Q}}_{w,ak} + \overline{\dot{Q}}_{w,ah} + \overline{\dot{Q}}_{w,AH} + \overline{\dot{Q}}_{w,k} + \overline{\dot{Q}}_{w,K} + \overline{\dot{Q}}_{w,H} + \overline{\dot{Q}}_{w,h}\right] \tag{21}$$

3. Results and Discussion

Table 1 shows the specification and the reference operating conditions of the VM heat pump simulated in this work. The wall temperatures of the hot heat exchanger, hot-side warm heat exchanger, cold-side warm heat exchanger and cold heat exchanger are 873K, 328K, 323K and 278K, respectively. Mean ope-

rating pressure is 40bar and operating frequency is 700rpm. The volumes of the cold active volume and the hot active volume vary with the phase shift of 90°.

Table 2 shows the simulated results at the reference operating conditions. The heat conduction losses through the hot regenerator and the hot displacer are larger than those through the cold regenerator and the cold displacer since the temperature difference between the hot heat exchanger and the warm heat exchanger is larger than that between the warm heat exchanger and the cold heat exchanger. Also, the pumping loss within the hot active volume is larger than that within the cold active volume since the temperature fluctuation within the hot active volume is larger than that within the cold active volume. But, the wall-to-gas heat transfers are larger in the cold active volume and the cold-side warm active volume than those in the hot active volume and the hot-side warm active volume.

Heat input to the hot heat exchanger is 934W and the net work done by the hot active volume to the hot displacer is 715W. It shows that only 715W out of 934W is converted from heat to work and is transferred to the hot displacer, and the remaining 219W is transferred to the hot-side warm active volume and the hot-side warm heat exchanger via heat conduction and the shuttle heat transfer. Since the cold active volume and the cold heat exchanger receive net heat from the cold-side warm active volume and the cold-side warm heat exchanger via heat conduction and the shuttle heat transfer, the net work done to the cold displacer by the cold active volume, 1736W, is larger than the net heat received by the cold heat exchanger, 1474W.

Table 1 Specification and reference operating conditions

	Unit	Hot Side	Warmh Side	Warmc Side	Cold Side
Working Volume					
Bore	[cm]	8.0			10.0
Stroke	[cm]	4.2			4.2
Appendix Gap	[cm]	0.1			0.1
Speed	[rpm]	700			
Mean Pressure	[bar]	40			
Phase Angle	[deg]	90			
Displacer Length	[cm]	12			16
Heat Exchanger					
Wall Temperature	[K]	873	328	323	278
Inner Tube Diameter	[cm]	0.6	0.2	0.2	0.2
Tube Length	[cm]	20	15	11	11
Number of Tubes		24	120	150	150
Regenerator					
Porosity		0.7			0.7
Length	[cm]	4			1.5

Table 2 Simulation results at reference operating condition

	Unit	Hot Side	$Warm_h$ Side	$Warm_c$ Side	Cold Side
HX Heat Transfer	[W]	934	-525	-1939	1474
P-V Work	[W]	715	-757	-1793	1736
Wall to Gas Heat Transfer at Working Volume	[W]	12.5	-3.5	-41.4	31.8
Pumping Loss	[W]	-42.7			18.8
Displacer Conduction	[W]	53.7		7.4	
Regenerator Conduction	[W]	65.3		9.1	
Heat Pump COP		2.40			
Refrigerator COP		1.44			

Table 3 Effects of various losses on performance

	Heat Exchanger Heat Transfer Rate [W]				COP_h	COP_c
	Hot	$Warm_h$	$Warm_c$	Cold		
Basic Model	852	-497	-2135	1678	2.76	1.76
Wall to Gas Heat Transfer at Working Volume	842	-489	-2090	1647	2.73	1.74
Regenerator Conduction	915	-558	-2129	1668	2.64	1.64
Displacer Conduction	902	-527	-2150	1669	2.66	1.66
Pumping loss	788	-415	-1919	1494	2.70	1.72
Internal losses	934	-525	-1939	1474	2.40	1.44
Internal losses+Shuttle +Wall Conduction	1773	-1358	-1824	1359	1.71	0.73

Effects of various losses on the performance of a VM heat pump are shown in Table 3. In basic model only limited heat transfer rates and the pressure drops within heat exchangers and regenerators are considered. Effects of the wall-to-gas heat transfer losses within the active volumes, regenerator conduction losses, displacer conduction losses and pumping losses, respectively, on the performance are also shown. Internal losses include all the losses listed above.

Net heat transfer rate for each heat exchanger, which is obtained when the pumping losses are added to the basic model, is smaller than that of the basic model. In basic model the appendix gaps between the cylinders and the displacers are not considered, whereas the appendix gaps are considered when the pumping losses are included. The amplitudes of the pressure fluctuations within the active volumes decrease since the volumes which are occupied by the working gases increase when the pumping losses are included. The decrease of the pressure fluctuation explains the decrease of net heat transfer rate for each heat exchanger. This result also shows that

the pumping loss within the hot active volume should be subtracted from the heat load of the hot heat exchanger rather than be added to the heat load of the hot heat exchanger as in the second-order analysis of a VM heat pump.

When the wall-to-gas heat transfer losses are added to the basic model the net heat transfer rate for each heat exchanger is smaller than that of the basic model since the walls of the active volumes behave like heat exchangers. It can be seen that the wall-to-gas heat transfer losses reduce the cooling and heating coefficients of performance.

The heat conduction losses through the regenerators and the displacers increase the net heat transfer rates of the hot heat exchanger and the warm heat exchangers, but decrease the net heat transfer rate of the cold heat exchanger.

When all internal losses are added into the basic model, the net heat input into the hot heat exchanger increases, but the heat input into the cold heat exchanger and the heat extracted from the warm heat exchangers decrease compared with those of the basic model. Hence, the internal losses reduce the performance of a VM heat pump. The internal losses reduce the heating and cooling coefficients of performance by 0.36 and 0.33, respectively. When external losses, such as the shuttle heat transfer losses and the conduction losses through the walls of the cylinders and regenerators, and the internal losses are added to the basic model, the heating and cooling coefficients of performance reduce by 1.05 and 1.03, respectively.

Table 4 compares the simulated results of the adiabatic analysis, the second-order analysis model(Choi and Jeong, 1996) and the third-order model of this study. In the adiabatic analysis only the losses generated by mixing are considered since the heat exchangers and the regenerators are assumed to be ideal. Predicted coefficients of performance of the second-order model and those of the third-order model are significantly lower than those of the adiabatic analysis, which shows that the performance of a VM heat pump is affected considerably by the losses. Predicted coefficients of the third-order model are slightly higher than those of the second-order model.

Figure 3 shows the volume change of the active volumes during a cycle. The pressure variations in the active volumes and the pressure difference between the active volumes during a cycle are shown in Fig.4 and Fig.5, respectively. The maximum pressure difference between the active volumes is about 10kPa, which is negligible compared with the mean pressure of 4,100kPa.

The mass flow rates through the interfaces between the control volumes are shown in Fig.6. The mass flow rates from the cold

Table 4 Comparison of 3rd-order analysis results with the results of 2nd-order analysis and adiabatic analysis

	Heat Exchanger Heat Transfer Rate [W]				COP_h	COP_c
	Hot	$Warm_h$	$Warm_c$	Cold		
Adiabatic Analysis	956	-511	-1952	1548	2.58	1.62
2nd-Order Analysis	1926	-1509	-1655	1041	1.64	0.54
3rd-Order Analysis	1773	-1358	-1824	1359	1.71	0.73

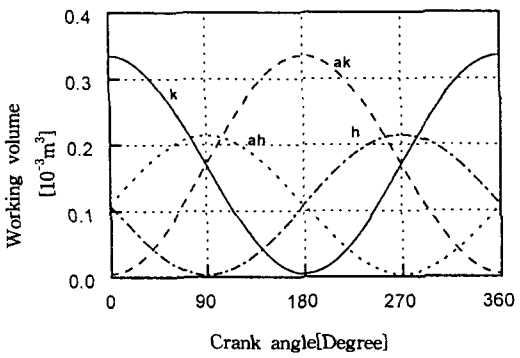

Fig.3 Working Volumes vs. crank angle

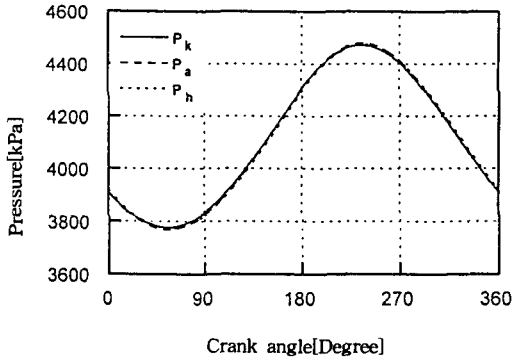

Fig.4 Working Volume Pressures vs. crank angle

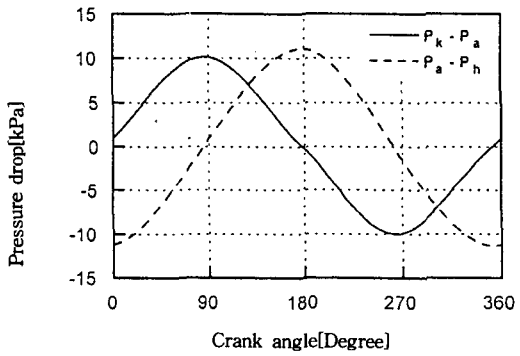

Fig.5 Pressure drops vs. crank angle

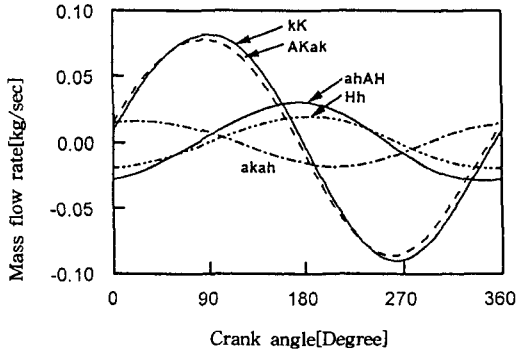

Fig.6 Mass flow rates vs. crank angle

active volume to the warm active volume reach their maxima when the crank angle is near 90°, at which the velocity of the cold displacer is maximum, while the mass flow rates from the warm active volume to the hot active volume reach their maxima when the crank angle is near 180°, at which the velocity of the hot displacer is maximum. Comparing with Fig.5 it can be seen that the mass flow rates from the cold active volume to the warm active volume have the same phase with that of the pressure difference between the cold active volume and the warm active volume, while the mass flow rates from the warm active volume to the hot active volume have the same phase with that of the pressure difference between the warm active volume and the hot active volume. Since the temperature of the cold active volume is lower than that of the hot active volume, the mass flow rates through the cold heat exchanger and the cold regenerator are larger than those through the hot heat, exchanger and the hot regenerator.

Figure 7 shows the temperature variations during a cycle within the active volumes and the heat exchangers. It can be seen that the amplitudes of the temperature fluctuations within the active volumes are larger than those of adjacent heat exchangers.

The temperatures of the working gases and the matrices within the regenerators are

shown in Fig.8. The temperature differences between the matrices and the working gases are very small. Heat is transferred form the matrices to the working gases within the cold regenerator from 0° to 180°, during which the mass flows from the cold active volume to the warm active volume as can be seen in Fig.6, since the temperatures of the working gases are lower than those of the matrices. Heat is transferred form the working gases to the matrices from 180° to 360°, during which the mass flows from the warm active volume to the cold active volume, since the temperatures of the working gases are higher than those of the matrices.

Figure 9 and 10 show the effect of rotational speed of the displacers on the heating capacity, cooling capacity and COP's when the mean pressure is 30bar, 40bar and 50bar, respectively. As mean pressure increases the heating and cooling capacities increase since the total mass of the working gas within a VM heat pump increases as mean pressure increases. COP's for cooling and heating increase because the effectivenesses of the heat exchangers and the regenerators increase due to the density increase of the working gas as mean pressure increases. For the same mean pressure cooling and heating capacities increase linearly as rotational speed increases, but COP's increase first and then decrease. Experimental results and the predictions of the third-order analysis by Kuehl et al.(1986) showed the same behavior. The rotational speed at which COP's are maxima decreases as mean pressure increases.

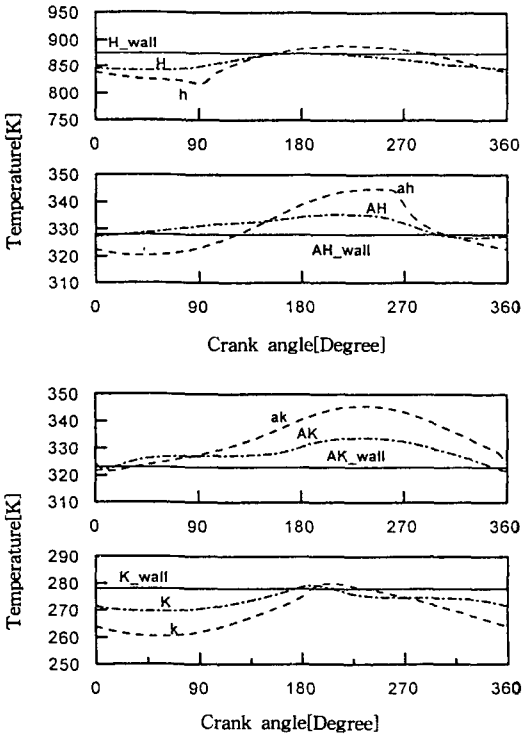

Fig.7 Gas and wall temperatures vs. crank angle

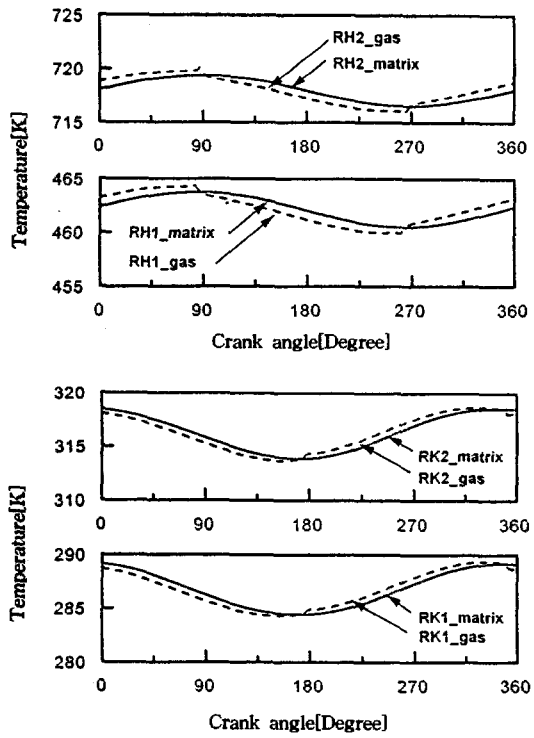

Fig.8 Regenerator matrix and gas temperatures vs. crank angle

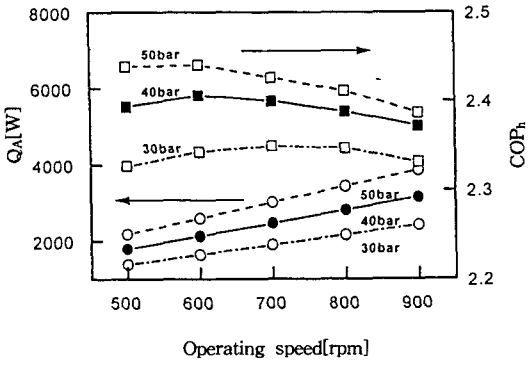

Fig.9 Heating capacity and COP_h vs. operating speed

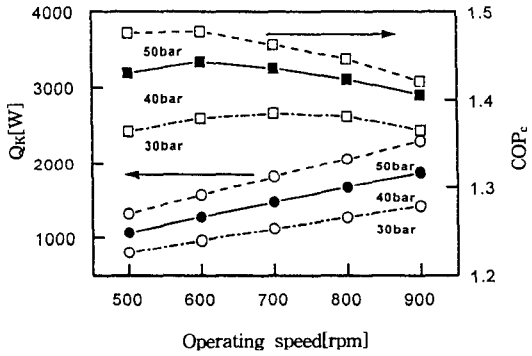

Fig.10 Cooling capacity and COP_c vs. operating speed

4. Conclusions

A third-order simulation model of a VM heat pump was presented. In this model the wall-to-gas heat transfer losses within the active volumes, the conduction losses through the regenerators and the displacers and the pumping losses were included in addition to the flow friction losses and the limited heat transfer losses, which have been considered in existing third-order models. Using the model thermodynamic behavior of the working gas was investigated and the effects of the various losses and operating parameters on the performance of a VM heat pump were shown.

The wall-to-gas heat transfer losses within the active volumes and the pumping losses reduce the cooling and heating capacities. The conduction losses through regenerators and the displacers increase the heating capacity and reduce the cooling capacity, but reduce the COP's for cooling and heating since they increase the heat input to the hot heat exchanger. Heating and cooling capacities and COP's increase as mean pressure increases. For the same mean pressure, heating and cooling capacities increase linearly as rotational speed increases, but COP's increase first and then decrease. The rotational speed at which COP's are maxima decrease as mean pressure increases.

References

(1) Kang, B. H., 1992, "Vuilleumier(VM) Cycle Heat Pumps", Air-conditioning and Refrigeration Engineering, Vol. 21, No. 1, pp. 19~25.

(2) Yoo, H. and , Kang, B. H., 1992, "Preliminary Design Conditions for a Thermally Actuated Refrigerator based on Vuilleumier Cycle", Korean Journal of KSME, Vol. 16, No. 12, pp. 2358~2367.

(3) Kuehl, H, D., Richter, N., and Schulz, S., 1986, "Computer Simulation of a Vuilleumier Cycle Heat Pump for Domestic Use", Proc. 21st IECEC, pp. 555~561.

(4) Carlsen, H., 1989, "Development of a Gas Fired Vuilleumier Heat Pump for Residential Heating", Proc. 24th IECEC, Washington, D.C., pp. 2257~2263.

(5) Sekiya, H. and Terada, F., 1991, "A Simulation Model for Vuilleumier Cycle Machines and Analysis of Characteristics", Journal of JSME(B), Vol. 57, No.

539, pp. 2449~2456.

(6) Yoo, H., 1989, "An Adiabatic Analysis on the Vuilleumier Refrigeration Cycle", Korean Journal of KSME, Vol. 13, No. 6, pp. 1231~1237.

(7) Choi, Y. S. and Jeong, E. S., 1996, "A Second-order Analysis of a VM Heat Pump", Air-conditioning and Refrigeration Engineering, Vol. 8, No. 2, pp. 208~218.

(8) Sherman, A., 1971, "Mathematical Analysis of a Vuilleumier Refrigerator", Proc. ASME Winter Meet., Paper 71-WA/HT-33.

(9) Kuehl, H. D. and Schulz, S., 1990, "Measured Performance of a Experimental Vuilleumier Heat Pump in Comparison to 3rd Order Theory", Proceedings of 25th IECEC, pp. 436~441.

(10) Choi, Y. S., Baik, J. H., Chang, H. M., and Jeong, E. S., 1994, "Proceedings of the Summer Annual Meeting of Air-conditioning and Refrigeration Engineers of Korea", pp. 286~296.

(11) Jeong, E. S. and Smith, J. L., Jr., 1992, "An Analytical Model of Heat Transfer with Oscillating Pressure", Proceedings of ASME National Heat Transfer Conference, pp. 97~104.

(12) Urieli, I. and Berchowitz, D. M., 1984, Stirling Cycle Analysis, Adam Hilger Ltd., Bristol.

(13) Tanaka, M., Yamashita, I., and Chisaka, F., 1989, "Flow and Heat Transfer Characteristics of Stirling Engine Regenerator in Oscillating Flow", JSME(B), Vol. 55, No. 516, pp. 2478~2475.